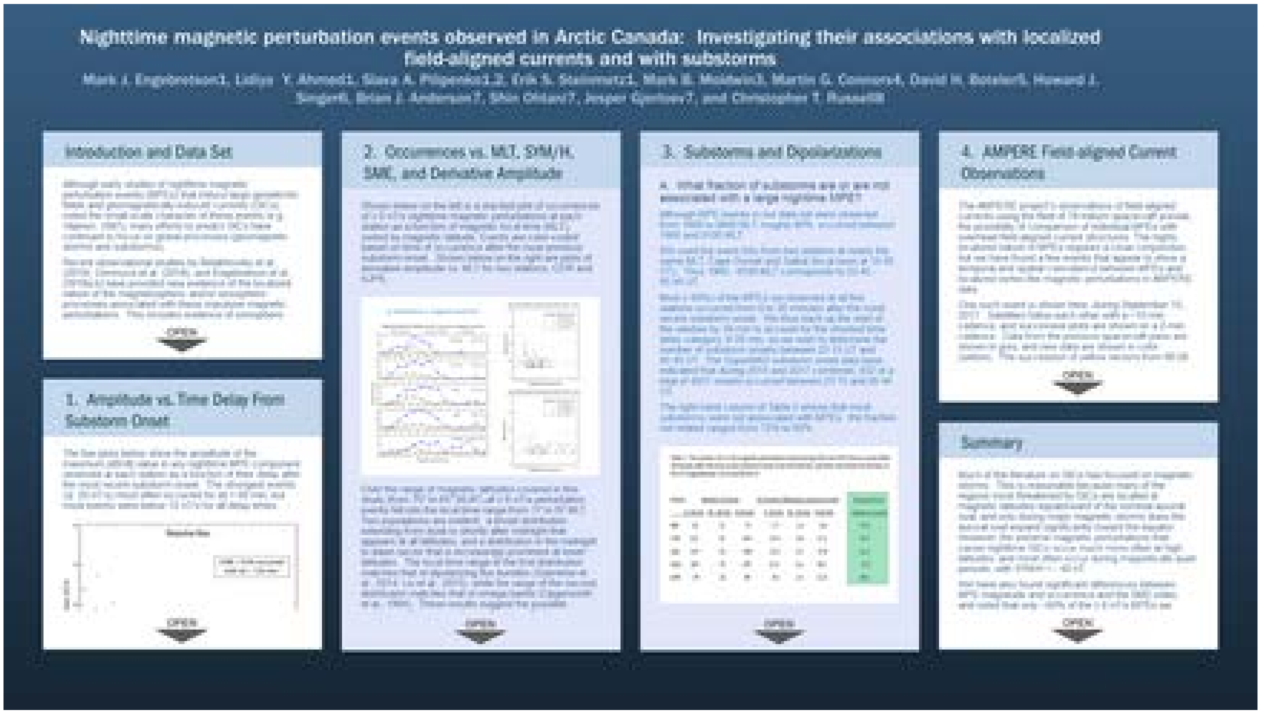

Nighttime magnetic perturbation events observed in Arctic Canada: Investigating their associations with localized field-aligned currents and with substorms

Mark J. Engebretson, Lidiya Y. Ahmed, Slava A. Pilipenko, Erik S. Steinmetz, Mark B. Moldwin, Martin G. Connors, David H. Boteler, Howard J. Singer, Brian J. Anderson, Shin Ohtani, Jesper Gjerloev, and Christopher T. Russell

Presented at:

The following is a link to the interactive HTML version of this e-Lightning poster:

https://agu2019fallmeeting-agu.ipostersessions.com/default.aspx?s=BD-27-3F-48-78-67-50-F3-B3-D7-43-E7-0B-4E-60-B1

Introduction and Data Set

Although early studies of nighttime magnetic perturbation events (MPEs) that induce large geoelectric fields and geomagnetically-induced currents (GICs) noted the small-scale character of these events (e.g., Viljanen, 1997), many efforts to predict GICs have continued to focus on global processes (geomagnetic storms and substorms).

Recent observational studies by Belakhovsky et al., (2019), Dimmock et al. (2019), and Engebretson et al., (2019a,b) have provided new evidence of the localized nature of the magnetospheric and/or ionospheric processes associated with these impulsive magnetic perturbations. This includes evidence of ionospheric current vortices, close association with poleward boundary intensifications and overhead auroral streamers, and the ~275 km effective radius of individual events. Individual events also displayed no close or consistent temporal correlation with substorm onsets.

Here we present additional analyses of a large number of nighttime MPEs that document lack of any close correlation between their occurrence and levels of the SME index, the SYM/H index, or of near-tail dipolarizations, and show that a substantial fraction of these events are not temporally associated with substorms.

We also show one example of a close temporal and spatial conjunction between an Iridium spacecraft and an extreme (34 nT/s) MPE observed in Arctic Canada that is consistent with the impact of a highly localized filamentary field-aligned current.

Our study is based on data from five stations, as detailed in Table 1 and the figure below (red circles). Also shown in the figure (yellow circle) is the northern magnetic footpoint of the geosynchronous GOES 13 spacecraft.

Table 1. Stations used in this study. Corrected magnetic (CGM) coordinates are for epoch 2015, using http:///sdnet.thayer.dartmouth.edu/aacgm/aacgm_calc.php#AACGM.

Array	Station Name	Code	GLAT	GLON	CGMLAT	CGMLON
MACCS	Repulse Bay	RBY	66.5°	273.8°	75.2°	-12.8°
	Cape Dorset	CDR	64.2°	283.4°	72.7°	3.0°
CANMOS	Iqaluit	IQA	63.8°	291.5°	71.4°	15.1°
AUTUMNX	Salluit	SALU	62.2°	284.3°	70.7°	4.1°
	Kuujuarapik	KJPK	55.3 °	282.2°	64.4°	0.2°

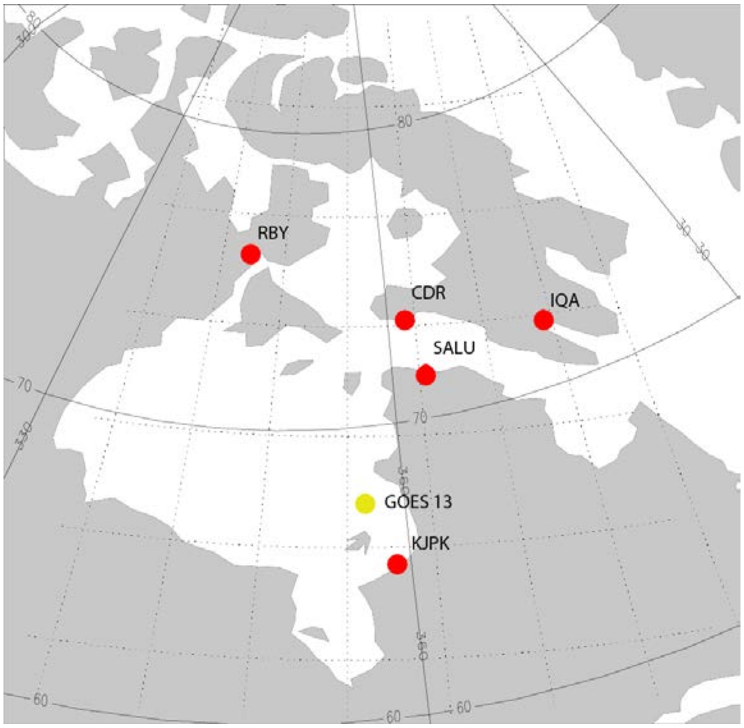

Table 2 shows the number of nighttime MPEs with derivative amplitude ≥ 6 nT/s at each of these stations during full years 2015 and 2017, Events are grouped into 3 categories of time delay after the most recent substorm onset listed in the SuperMAG substorm list.

Table 2. Numbers of nighttime perturbation events observed at each station with derivative amplitude |dBx/dt| ≥ 6 nT/s in any component, as a function of Δt.

Station	MLAT	Δt ≤ 30 min		30 < Δt < 60 min		Δt ≥ 60 min		All
		#	%	#	%	#	%	#
RBY	75.2°	53	60	22	25	13	15	88
CDR	72.7°	112	67	32	19	22	13	166
IQA	71.4°	119	66	29	16	32	18	180
SALU	70.7°	187	66	47	17	48	17	282
KJPK	64.4°	79	64	20	16	25	20	124

Events with Δt ≤ 30 min were most likely to be associated with substorm processes, while those with Δt ≧ 60 min (and up to several days) were not. The fractions of events that occurred in the three different delay ranges remained roughly constant at all stations.

Note, too, that the number of events peaked at Salluit (70.7° MLAT), and was lowest at the two latitude extremes: Repulse Bay (75.2° MLAT) and Kuujuarapik (64.7° MLAT).

1. Amplitude vs. Time Delay From Substorm Onset

The five plots below show the amplitude of the maximum |dB/dt| value in any nighttime MPE component observed at each station as a function of their delay after the most recent substorm onset. The strongest events (≧ 20 nT/s) most often occurred for Δt < 60 min, but most events were below 12 nT/s for all delay times.

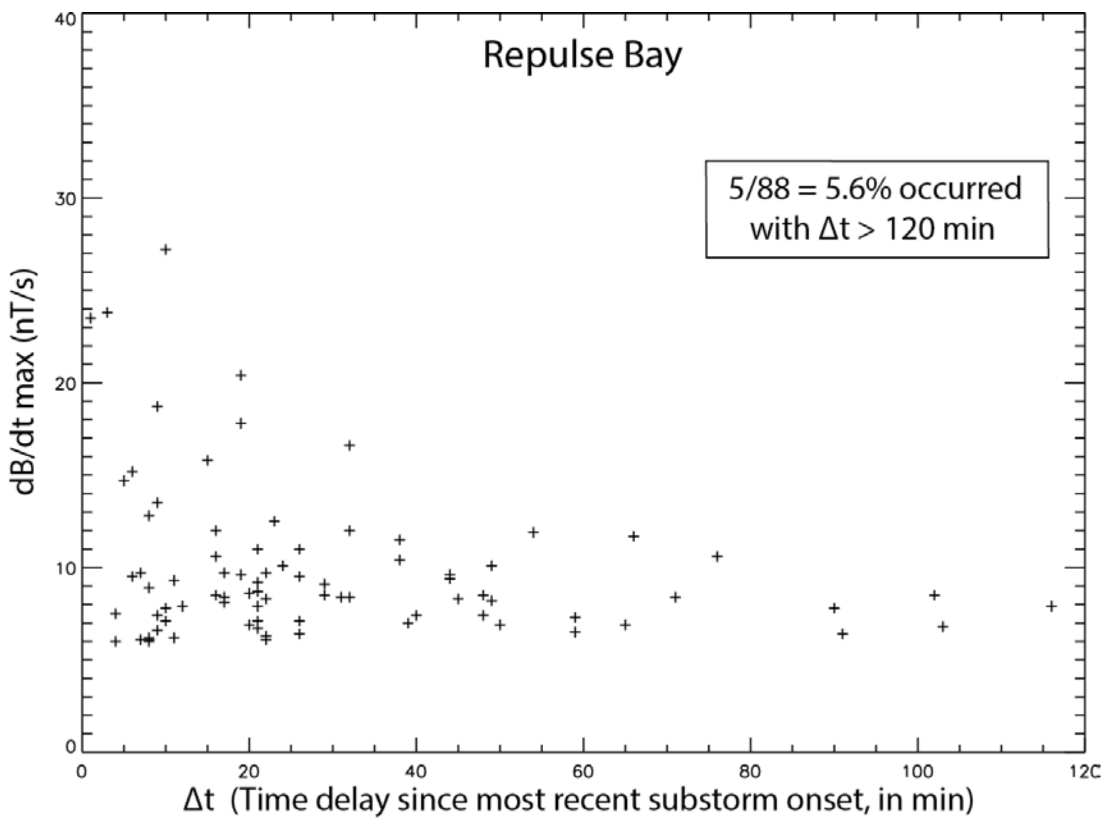

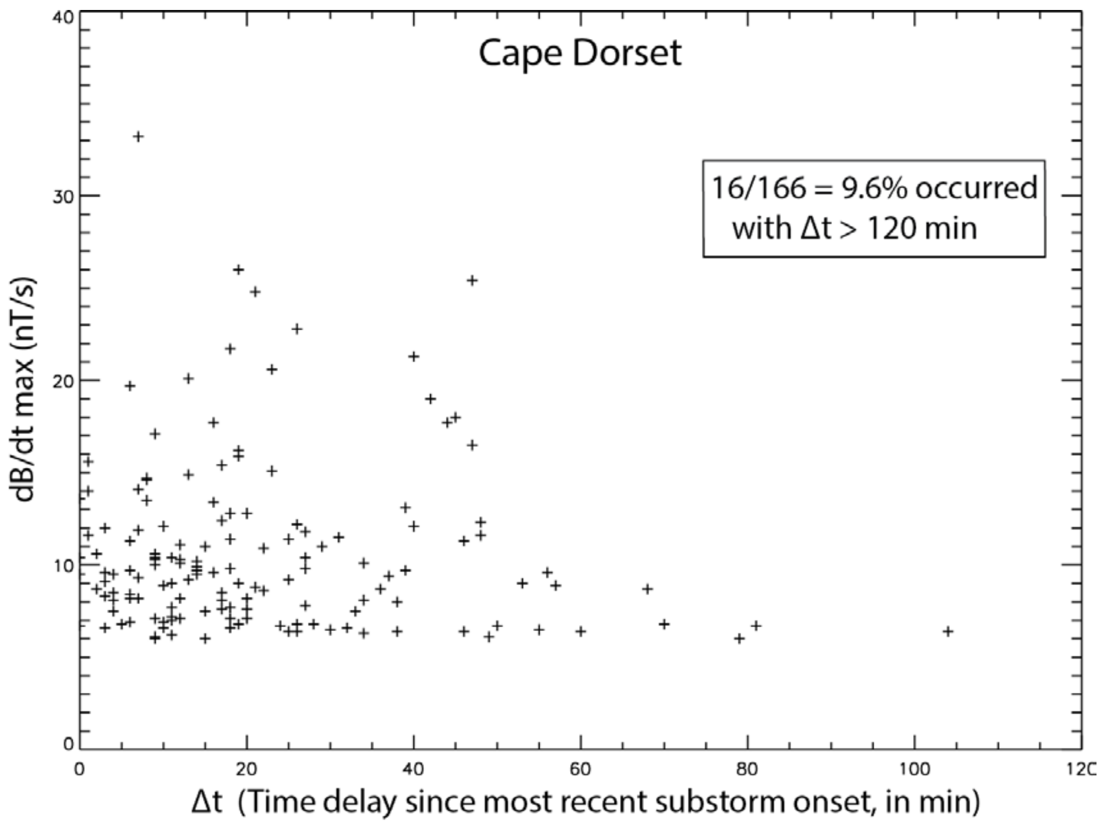
Cape Dorset
16/166 = 9.6% occurred
with Δt > 120 min
dB/dt max (nT/s)
0
10
20
30
40
0
20
40
60
80
100
12C
Δt (Time delay since most recent substorm onset, in min)

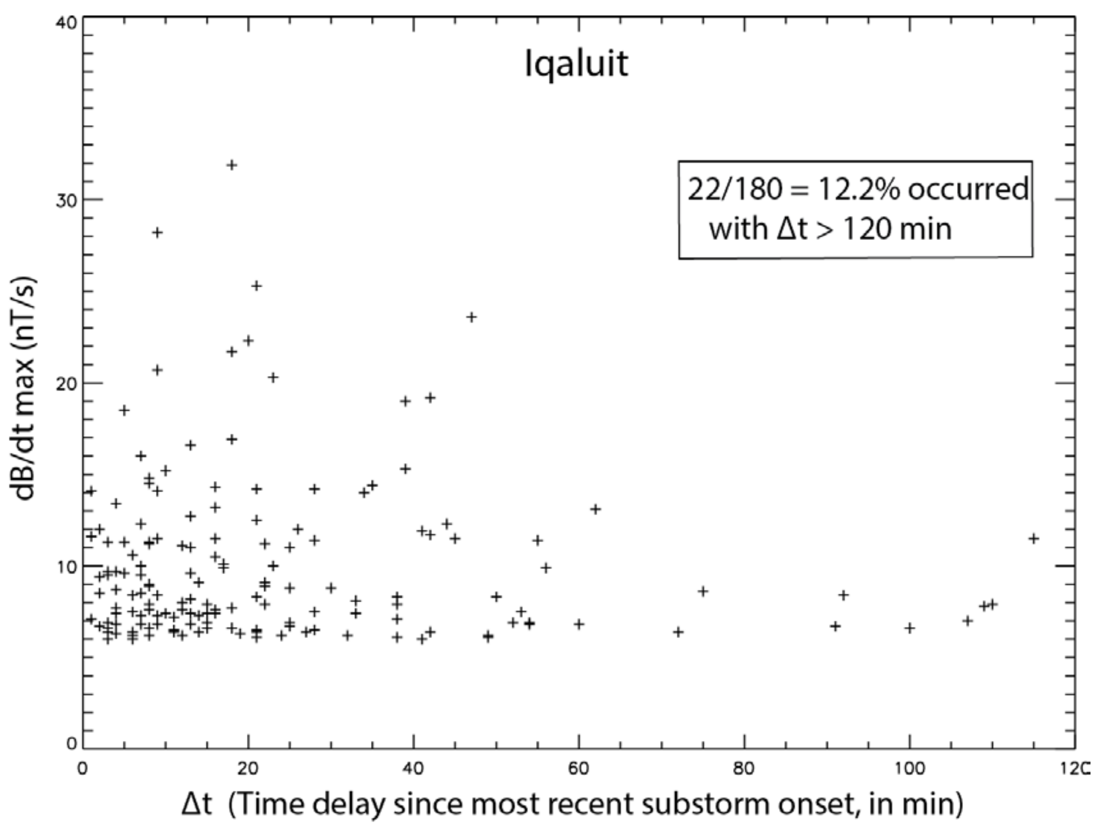
Iqaluit
22/180 = 12.2% occurred
with Δt > 120 min
dB/dt max (nT/s)
0
10
20
30
40
0
20
40
60
80
100
12C
Δt (Time delay since most recent substorm onset, in min)

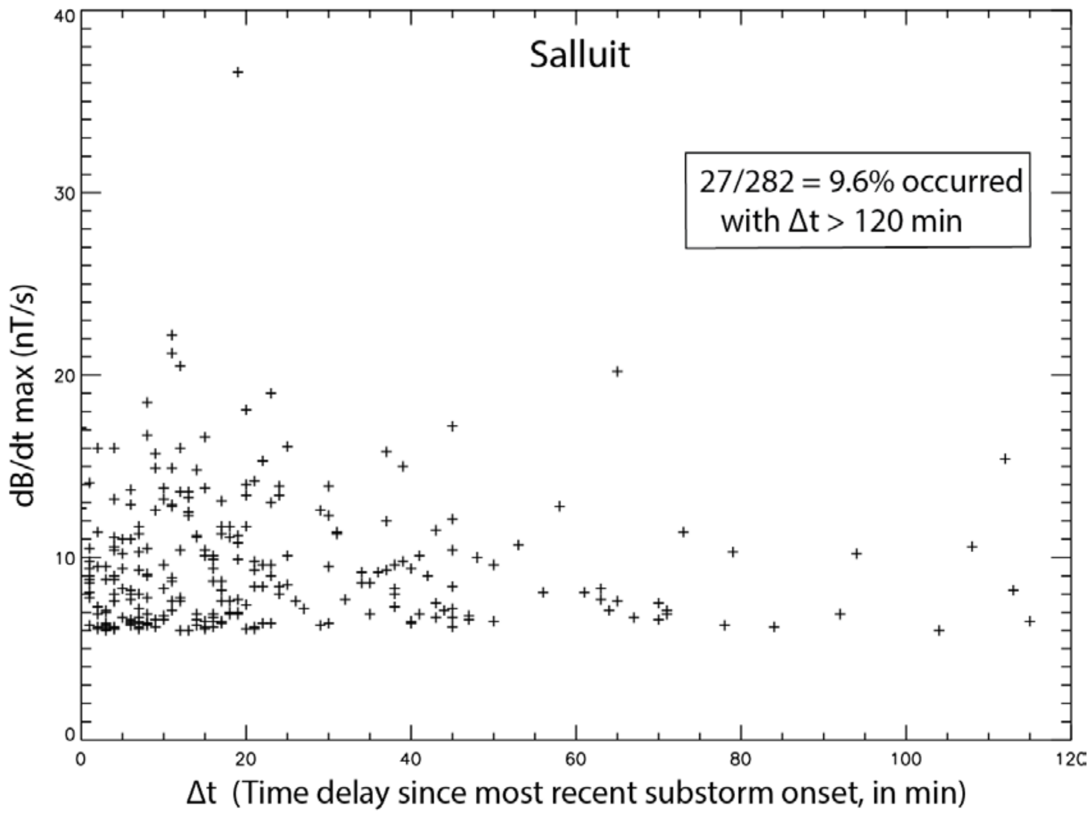
Salluit
27/282 = 9.6% occurred
with Δt > 120 min
dB/dt max (nT/s)
0
10
20
30
40
0
20
40
60
80
100
120
Δt (Time delay since most recent substorm onset, in min)

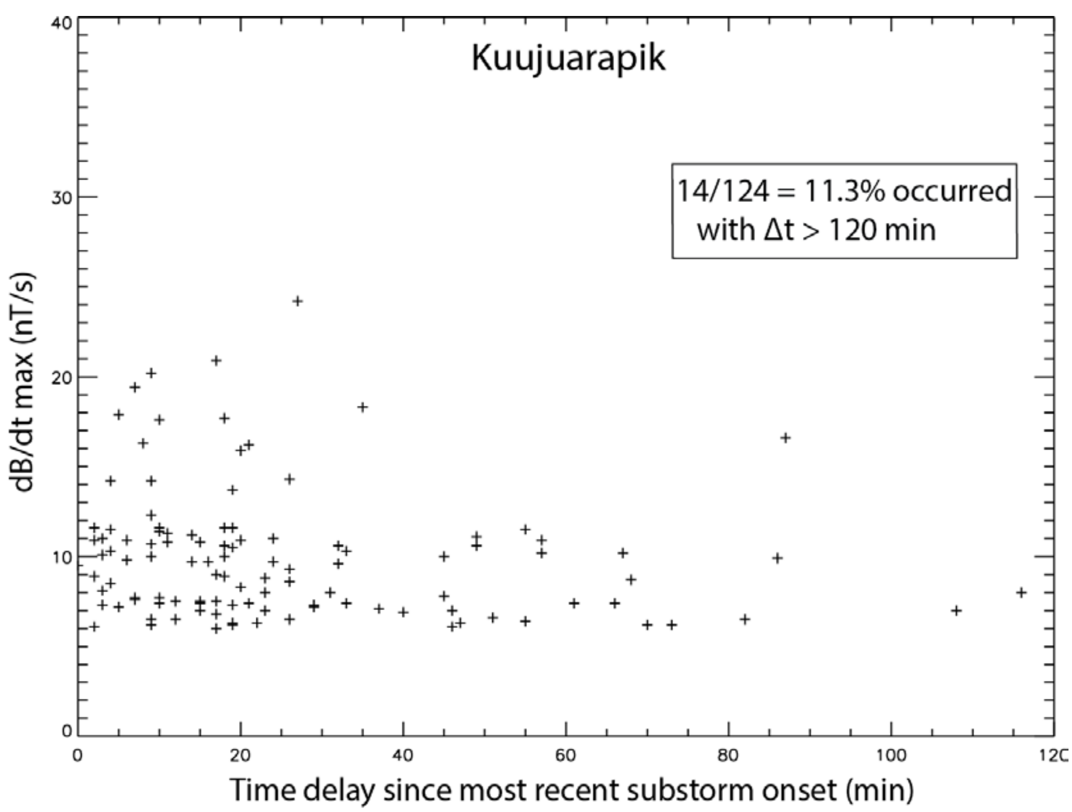
Kuujuarapik
14/124 = 11.3% occurred
with Δt > 120 min
dB/dt max (nT/s)
0
10
20
30
40
0
20
40
60
80
100
120
Time delay since most recent substorm onset (min)

2. Occurrences vs. MLT, SYM/H, SME, and Derivative Amplitude

Shown below on the left is a stacked plot of occurrences of ≥ 6 nT/s nighttime magnetic perturbations at each station as a function of magnetic local time (MLT), sorted by magnetic latitude. Events are color-coded based on time of occurrence after the most previous substorm onset. Shown below on the right are plots of derivative amplitude vs. MLT for two stations, CDR and KJPK.

A. Distribution vs. magnetic local time

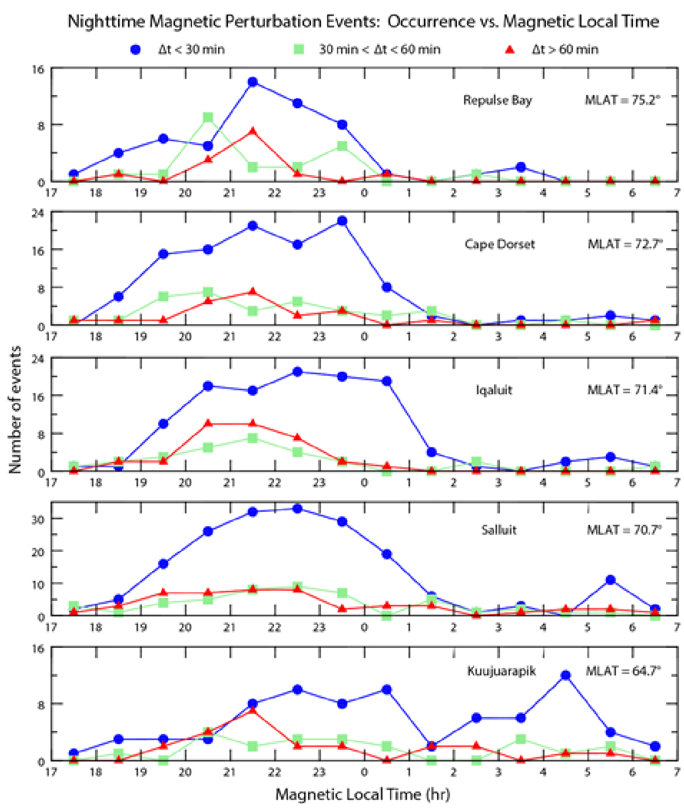

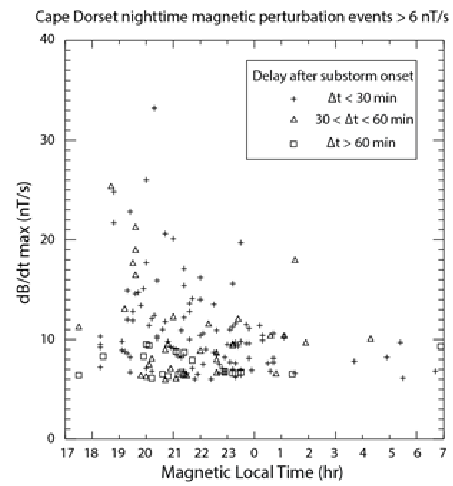

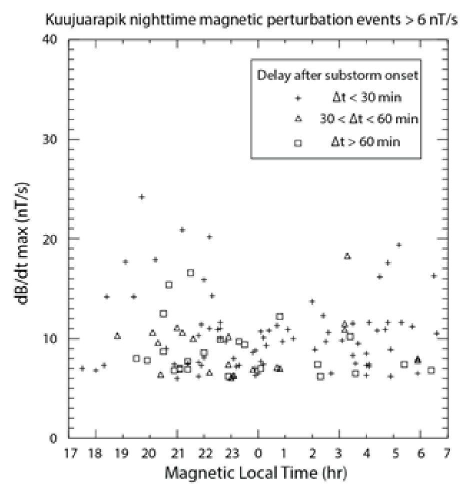

Over the range of magnetic latitudes covered in this study (from 75° to 65° MLAT) all ≥ 6 nT/s perturbation events fell into the local time range from 17 to 07 MLT. Two populations are evident: a broad distribution extending from dusk to shortly after midnight that appears at all latitudes, and a distribution in the midnight to dawn sector that is increasingly prominent at lower latitudes. The local time range of the first distribution matches that of dipolarizing flux bundles (Gabrielse et al., 2014; Liu et al., 2015), while the range of the second distribution matches that of omega bands (Opgenoorth et al., 1994). These results suggest the possible existence of two separate mechanisms that can generate these impulsive events.

As Table 3 shows, the time delay distributions were similar for pre- and post-midnight events. Post-midnight events were slightly more likely to occur within 30 min after substorm onsets than pre-midnight events (70% vs. 66%), and less likely to occur more than 60 minutes after onset (12% vs. 17%).

Table 3. Distribution of pre- and post-midnight events as a function of time between the most recent substorm onset and event occurrence.
Pre-midnight events: from 17.5 to 0.5 hours MLT, Post-midnight events: from 2.5 to 6.5 MLT

Pre-midnight

Station	RB		CD		IQ		SA		KU	
	#	%	#	%	#	%	#	%	#	%
t ≤ 30 min	50	60	105	69	107	65	168	69	46	59
30-60 min	20	24	28	18	24	15	37	15	15	19
t ≥ 60 min	13	16	20	13	34	21	39	16	17	22
Total	83		153		165		244		78	

Combined: t ≤ 30 min: 66%, 30-60 min: 17%, t ≥ 60 min: 17%

Post-midnight

Station	RB		CD		IQ		SA		KU	
	#	%	#	%	#	%	#	%	#	%
t < 30 min	3	75	5	71	7	70	17	61	30	75
30-60 min	1	25	1	14	3	30	5	18	6	15
t > 60 min	0	0	1	14	0	0	6	21	4	10
Total	4		7		10		28		40	

Combined: t ≤ 30 min: 70%, 30-60 min: 18%, t ≥ 60 min: 12%

Table 4 shows that the vast majority of post-midnight events at the lowest latitude station (KJPK) followed multiple substorm onsets within a 2-hour interval, and many of these events occurred within a few minutes of each other. However, the derivative amplitude did not vary with the number of prior onsets.

Table 4: The number of substorm onsets within 2 hours prior to a large perturbation event (|dB/dt| > 6 nT/s) occurring at Kuujuarapik between 03:00 and 07:00 MLT.

Number of Onsets	0	1	2	3	4	5	6
Number of Days	1	2	8	7	4	0	1
Number of Events	2	2	15	11	7	0	2
Amplitude							
Minimum	6.8	6.5					9.5
Median			9.0	10.8	9.8		
Maximum	8.1	7.3					11.5

B. Distribution vs. SYM/H

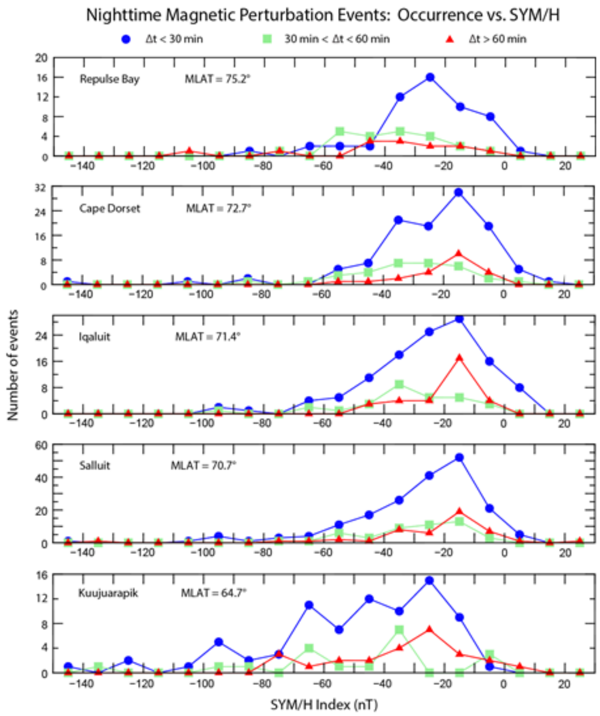

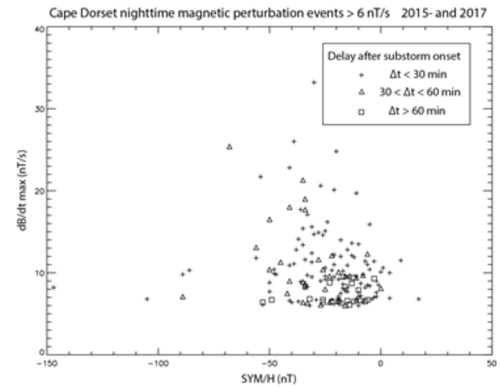

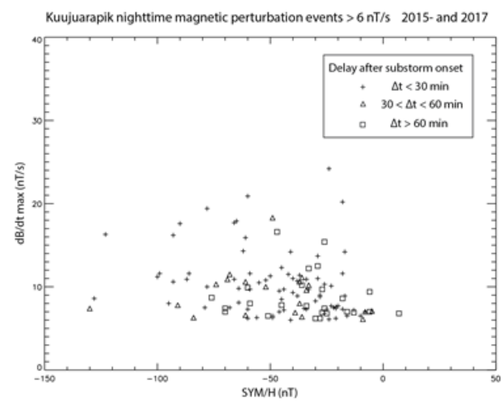

At all stations the occurrence distributions peaked near SYM/H ~ -20 nT, and above 72° MLAT nearly all events occurred when SYM/H was between -40 and +10 nT. The tail of the distribution at more negative SYM/H values increased significantly at the lowest latitude station (64.7° MLAT). This most likely reflects the equatorward expansion of the auroral oval during geomagnetic storms. The occurrence distributions for the three time delay categories were roughly similar at each station.

The plots at the right show that there was essentially no correlation between derivative amplitude and SYM/H value at either CDR or KJPK.

C. Distribution vs. SME

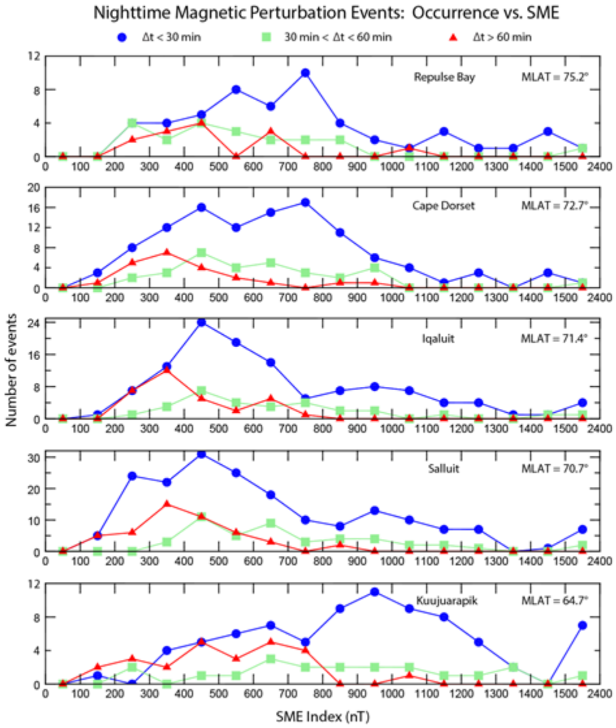

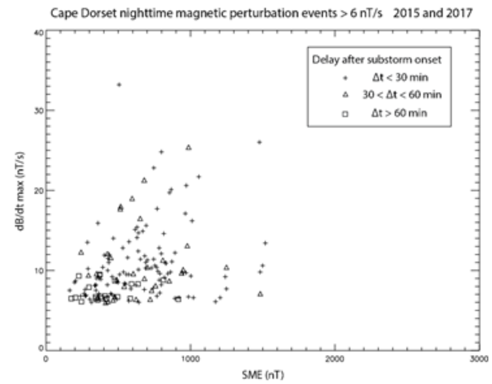

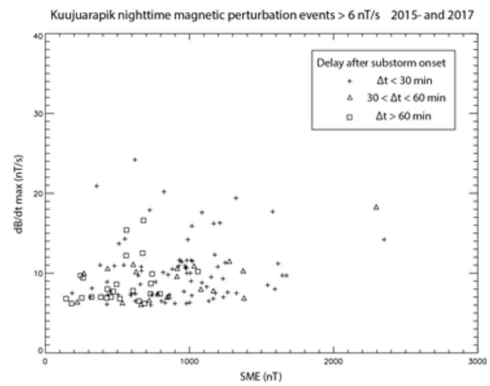

Large perturbation events occurred over a wide range of SME values (the SuperMAG version of the AE index) at all stations. Very few events occurred at any station for SME < 200 nT. Only at the lowest latitude station (Kuujuarapik) did most events occur for SME > 800 nT – but fewer events occurred for high SME there than at Salluit (70.7° MLAT). The occurrence distributions for the three time delay categories were again roughly similar at each station.

There was only a modest correlation between the derivative amplitude and the SME index: the amplitude of the most intense events increased with SME at Cape Dorset, but not at Kuujuarapik, and most events at all SME values and all three time ranges were below 12 nT/s. Only 7 of the 842 total events occurred when SME exceeded 2000 nT.

D. Distribution vs. Derivative Amplitude

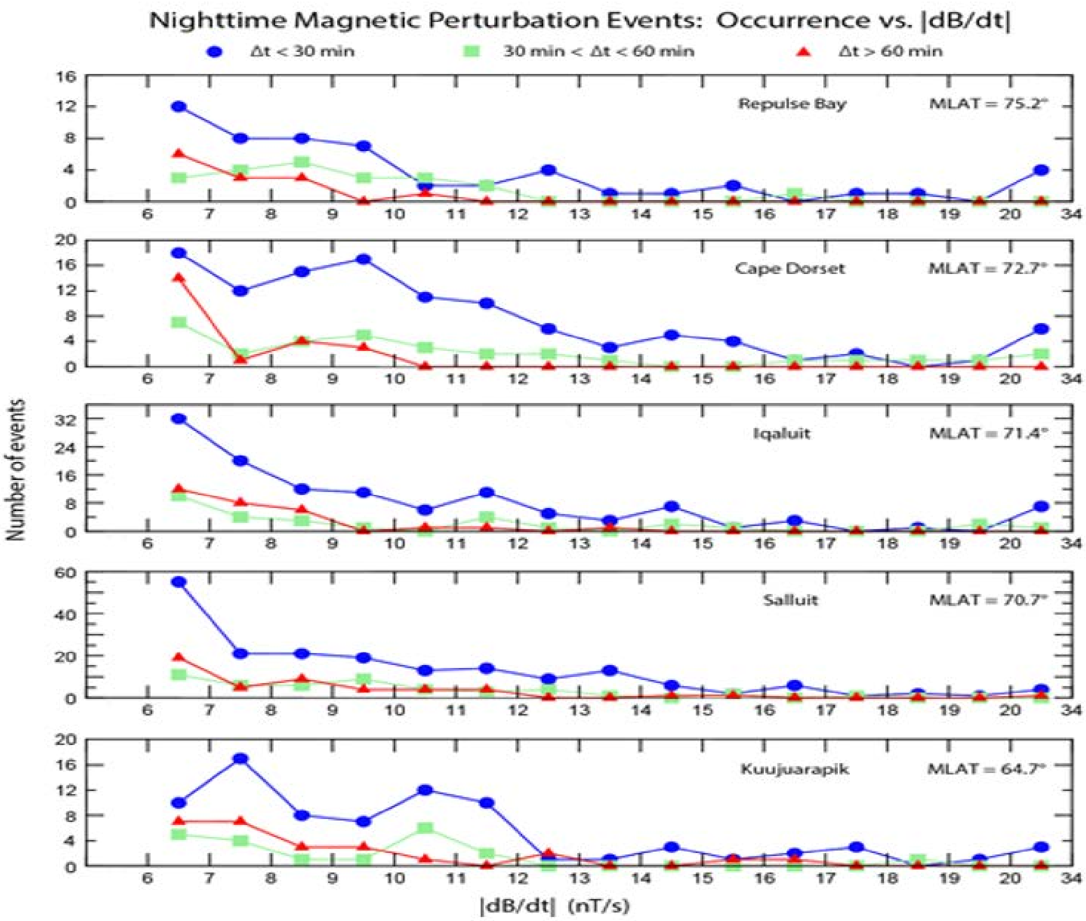

At all five stations and in all three time delay categories event occurrences fell off roughly monotonically from a peak between 6 and 7 nT/s to higher values, with no clear latitudinal trend. (Note that the last interval at the right includes all events with amplitude > 20 nT/s.)

3. Substorms and Dipolarizations

A. What fraction of substorms are or are not associated with a large nightime MPE?

Although MPE events in our data set were observed from 1600 to 0600 MLT, roughly 80% occurred between 1900 and 0100 MLT.

We used the event lists from two stations at nearly the same MLT, Cape Dorset and Salluit (local noon at 16:45 UT). Thus 1900 - 0100 MLT corresponds to 23:45 - 05:45 UT.

Most (~60%) of the MPEs we observed at all five stations occurred from 0 to 30 minutes after the most recent substorm onset. We thus back up the start of the window by 30 min to account for the shortest time delay category, 0-30 min, so we wish to determine the number of substorm onsets between 23:15 UT and 05:45 UT. The SuperMAG substorm onset data base indicated that during 2015 and 2017 combined, 932 of a total of 4031 onsets occurred between 23:15 and 05:45 UT.

The right-hand column of Table 5 shows that most substorms were not associated with MPEs: the fraction not related ranged from 72% to 92%.

Table 5. The number of ≥ 6 nT/s magnetic perturbation events during 2015 and 2017 that occurred within 30 minutes after the most recent substorm onset, from 30 to 60 min, and their sum (from 0 to 60 min), in the UT range between 23:15 and 05:45 UT.

Station	Number of Events			% of events following a substorm onset			SS onset % not related to events
	0-30 min	30 - 60 min	0-60 min	0-30 min	30 - 60 min	0-60 min	
RBY	53	22	75	5.7	2.4	8.0	92.0
CDR	112	32	144	13.4	3.8	17.3	82.7
IQA	119	29	148	14.3	3.5	17.8	82.2
SALU	187	47	234	22.5	5.6	28.1	71.9
KJPK	79	20	99	9.5	2.4	11.9	88.1

B. Multiple-Onset Substorms: How Important are they for GICs?

Using MPE events at Iqaluit and Salluit with ≥ 6 nT/s derivatives as proxies for GICs, we tabulated the number of their occurrences as a function of the number of substorm onsets that occurred within 2 hours prior to the MPE.

Table 6 shows that a disproportionately large number of events with SME > 1000 nT occurred during multiple-onset groupings of substorms, and very few during isolated substorms or long after the most recent substorm.

In contrast, there was little dependence of large dB/dt events on the number of prior onsets, and nearly 20% occurred more than 2 hours after the most recent substorm.

Table 6. The number of MPEs observed at Salluit and Iqaluit during 2015 and 2017, as a function of the number of substorm onsets (from the SuperMAG database) that occurred within 2 hours prior to the MPE: all events, events with SME > 1000 nT, and events with dB/dt > 10 nT.

Number of Onsets	Total MPE Events		SME > 1000				dB/dt > 10 nT			
	Salluit	Iqaluit	Salluit		Iqaluit		Salluit		Iqaluit	
	#	#	#	%	#	%	#	%	#	%
0	27	22	0	0	0	0	5	19	4	18
1	124	78	7	6	2	3	60	48	17	22
2	85	47	10	12	7	15	37	44	22	47
3	33	20	12	61	8	40	15	45	10	50
4	11	7	7	64	6	86	10	91	1	14
5	1	0	1	100	0	--	0	--	0	- -

C. Relation to Dipolarizations at Synchronous Orbit

In each of the three case studies of MPEs presented by Engebretson et al. (2019b) that occurred within 30 min of a substorm onset, rapid increases of from 15 to 30 nT in the Bz component of the magnetic field (dipolarizations) at GOES 13 coincided with an MPE to within a few minutes. The figure below presents a comparison of the GOES 13 dipolarizations observed within 15 minutes of all the MPEs observed at Repulse Bay during 2015 and 2017, grouped in two categories: 52 MPEs occurring within 30 minutes of the most recent substorm onset, and 14 occurring more than 60 minutes after onset.

Nearly all of the Δt ≤ 30 min dipolarizations were positive, and many exceeded 20 nT, while only small amplitudes were observed for the Δt ≥ 60 min events. Extending the dipolarization time range from 15 min to 45 min, we found that dipolarizations of ≥ 20 nT amplitude at GOES 13 occurred prior to 73% of the Δt ≤ 30 min MPEs but only 29% of the Δt ≥ 60 min MPEs.

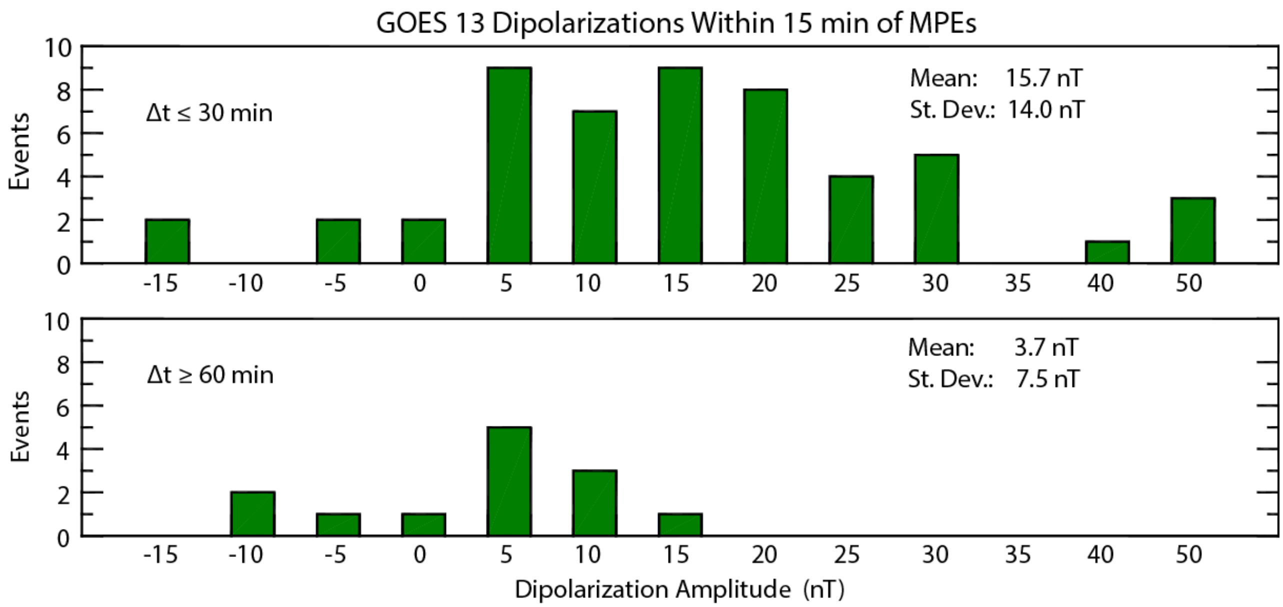

4. AMPERE Field-aligned Current Observations

The AMPERE project's observations of field-aligned currents using the fleet of 78 Iridium spacecraft provide the possibility of comparison of individual MPEs with overhead field-aligned current structures. The highly localized nature of MPEs requires a close conjunction, but we have found a few events that appear to show a temporal and spatial coincidence between MPEs and localized vortex-like magnetic perturbations in AMPERE data.

One such event is shown here, during September 15, 2017. Satellites follow each other with a ~10 min cadence, and successive plots are shown on a 2-min cadence. Data from the previous spacecraft pass are shown in grey, and new data are shown in color (yellow). The succession of yellow vectors from 00:28 to 00:34 UT shows a localized counterclockwise rotation of dB during the northward passage of a spacecraft very nearly overhead of Salluit (black dot), where an extremely large MPE was observed. Peak derivatives in all 3 component occurred between 00:31 and 00:33 UT. Such a vortical structure is consistent with a large but localized filamentary field-aligned current.

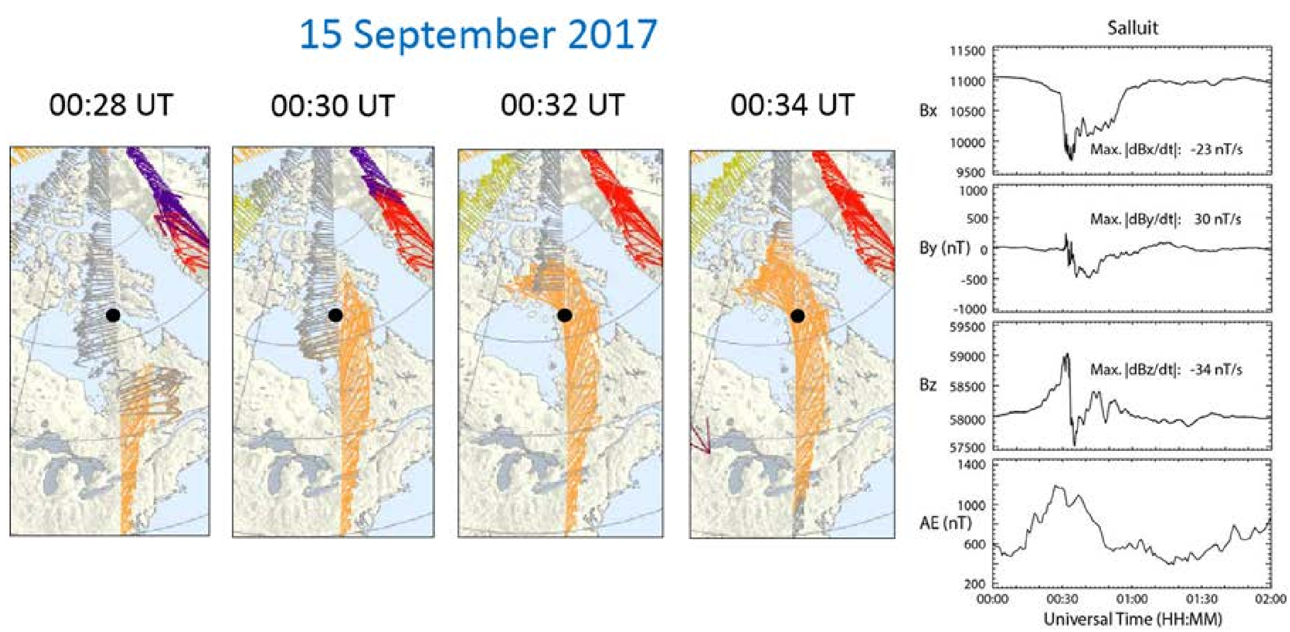

Summary

Much of the literature on GICs has focused on magnetic storms. This is reasonable because many of the regions most threatened by GICs are located at magnetic latitudes equatorward of the nominal auroral oval, and only during major magnetic storms does the auroral oval expand significantly toward the equator. However, the extreme magnetic perturbations that cause nighttime GICs occur much more often at high latitudes, and most often occur during magnetically quiet periods, with SYM/H > - 40 nT.

We have also found significant differences between MPE magnitude and occurrence and the SME index, and noted that only ~60% of the ≥ 6 nT/s MPEs we observed occurred within 30 minutes of the most recent substorm onset. A recent study by Freeman et al. (2019) found a similar result. They noted that in data from 3 stations in the UK over two solar cycles (only) 54–56% of all extreme rate of change values occurred during substorm expansion or recovery phases.

The main implication of this study is that neither a magnetic storm nor a substorm is a necessary or sufficient condition for the occurrence of the extreme nighttime magnetic perturbation events that can cause GICs.

Instead, both early and recent studies point to localized processes in the magnetotail, which often occur during substorms but can also occur at other times, as being responsible for generating these events. We intend to investigate the associations between MPEs and these processes in future studies. In particular, preliminary superposed epoch results indicate a good temporal correlation between MPEs and instances of negative but rising IMF Bz values.

Disclosures

Work at Augsburg University and the University of Michigan was supported by National Science Foundation grants AGS-1651263 and AGS-1654044.

CV

(1) Augsburg University, Minneapolis, MN; (2) Institute of Physics of the Earth, Moscow, Russia; (3) University of Michigan, Ann Arbor, MI; (4) Athabasca University, Athabasca, AB, Canada; (5) Natural Resources Canada, Ottawa, ON, Canada; (6) NOAA Space Weather Prediction Center, Boulder, CO; (7) JHU/APL, Laurel, MD; (8) UCLA, Los Angeles, CA

Abstract

The rapid changes of magnetic fields associated with nighttime magnetic perturbations with amplitudes |ΔB| of hundreds of nT and 5-10 min periods can induce bursts of geomagnetically-induced currents that can harm technological systems. Recent studies of these events in eastern Arctic Canada, based on data from four ground magnetometer arrays and augmented by observations from auroral imagers and high-altitude spacecraft in the nightside magnetosphere, showed them to be highly localized, with largest |dB/dt| values within a ~275 km half-maximum radius that was associated with a region of shear between upward and downward field-aligned currents, and usually but not always associated with substorms. In this study we look in more detail at the field-aligned currents associated with these events using AMPERE data, and compare the context and characteristics of events not associated with substorms (occurring from 60 min to over two days after the most recent substorm onset) to those occurring within 30 min of onset. Preliminary results of this comparison, based on events with |dB/dt|≥ 6 nT/s observed during 2015 and 2017 at Repulse Bay (75.2° CGMLAT), showed that the SYM/H distributions for both categories of events were similar, with 85% between -40 and 10 nT, and the SME values during non-substorm events coincided with the lower half of the range of SME values for events during substorms (200 – 700 nT). Dipolarizations of ≥ 20 nT amplitude at GOES 13 occurred within 45 minutes prior to 73% of the substorm events but only 29% of the non-substorm events. These observations suggest that predictions of GICs cannot focus solely on the occurrence of intense substorms.

REFERENCES

Belakhovsky, V. B. et al. (2018), Characteristics of the variability of a geomagnetic field for studying the impact of the magnetic storms and substorms on electrical energy systems, Izvestiya, Physics of the Solid Earth, 54, 52–65, doi:10.1134/S1069351318010032

Dimmock, A. P. et al. (2019), The GIC and geomagnetic response over Fennoscandia to the 7-8 September 2017 geomagnetic storm, Space Weather, 17, 989 –1010, doi:10.1029/2018SW002132

Engebretson, M. J. et al. (2019a), Nighttime magnetic perturbation events observed in Arctic Canada: 1. Survey and statistical analysis, Journal of Geophysical Research: Space Physics, 124, 7442–7458, doi: 10.1029/2019JA026794

Engebretson, M. J. et al. (2019b), Nighttime magnetic perturbation events observed in Arctic Canada: 2. Multiple-instrument observations, Journal of Geophysical Research: Space Physics, 124, 7459-7476, doi:10.1029/2019JA026797

Freeman, M. P., C. Forsyth, and I. J. Rae (2019), The influence of substorms on extreme rates of change of the surface horizontal magnetic field in the United Kingdom, Space Weather, 17, 827 –844, doi:10.1029/2018SW002148

Gabrielse, C., V. Angelopoulos, A. Runov, and D. L. Turner (2014), Statistical characteristics of particle injections throughout the equatorial magnetotail, Journal of Geophysical Research: Space Physics, 119, 2512–2535, doi:10.1002/2013JA019638

Liu, J., V. Angelopoulos, X. Chu, X.-Z. Zhou, and C. Yue (2015), Substorm Current Wedge Composition by Wedgelets. Geophysical Research Letters, 42, 1669–1676, doi:10.1002/2015GL063289

Opgenoorth, H. J., M. A. L. Persson, T. I. Pulkkinen, and R. J. Pellinen (1994), Recovery phase of magnetospheric substorms and its association with morning-sector aurora, Journal of Geophysical Research, 99, 4115-4129, doi:10.1029/93JA01502

Viljanen, A., (1997), The relation between geomagnetic variations and their time derivatives and implications for estimation of induction risks, Geophysical Research Letters, 24, 631–634, doi:10.1029/97GL00538